



Compartmentalized Reconstitution of Post-squalene Pathway for 7-Dehydrocholesterol Overproduction in *Saccharomyces cerevisiae*

Xiao-Jing Guo^{1,2}, Ming-Dong Yao^{1,2}, Wen-Hai Xiao^{1,2}, Ying Wang^{1,2*}, Guang-Rong Zhao^{1,2} and Ying-Jin Yuan^{1,2}

¹ Frontier Science Center for Synthetic Biology and Key Laboratory of Systems Bioengineering (Ministry of Education), School of Chemical Engineering and Technology, Tianjin University, Tianjin, China, ² Collaborative Innovation Center of Chemical Science and Engineering (Tianjin), Tianjin University, Tianjin, China

OPEN ACCESS

Edited by:

Daniela De Biase,
Sapienza University of Rome, Italy

Reviewed by:

Han Xiao,
Shanghai Jiao Tong University, China
Gianluca Bleva,
Institute of Sciences of Food
Production, Italian National Research
Council, Italy

*Correspondence:

Ying Wang
ying.wang@tju.edu.cn

Specialty section:

This article was submitted to
Microbial Physiology and Metabolism,
a section of the journal
Frontiers in Microbiology

Received: 04 February 2021

Accepted: 06 April 2021

Published: 21 May 2021

Citation:

Guo X-J, Yao M-D, Xiao W-H,
Wang Y, Zhao G-R and Yuan Y-J
(2021) Compartmentalized
Reconstitution of Post-squalene
Pathway for 7-Dehydrocholesterol
Overproduction in *Saccharomyces*
cerevisiae.

Front. Microbiol. 12:663973.
doi: 10.3389/fmicb.2021.663973

7-Dehydrocholesterol (7-DHC) is the direct precursor to manufacture vitamin D₃. Our previous study has achieved 7-DHC synthesis in *Saccharomyces cerevisiae* based on the endogenous post-squalene pathway. However, the distribution of post-squalene enzymes between the endoplasmic reticulum (ER) and lipid bodies (LD) might raise difficulties for ERG proteins to catalyze and deliver sterol intermediates, resulting in unbalanced metabolic flow and low product yield. Herein, we intended to rearrange the subcellular location of post-squalene enzymes to alleviate metabolic bottleneck and boost 7-DHC production. After identifying the location of DHCR24 (C-24 reductase, the only heterologous protein for 7-DHC biosynthesis) on ER, all the ER-located enzymes were grouped into four modules: ERG1/11/24, ERG25/26/27, ERG2/3, and DHCR24. These modules attempted to be overexpressed either on ER or on LDs. As a result, expression of LD-targeted DHCR24 and ER-located ERG1/11/24 could promote the conversion efficiency among the sterol intermediates to 7-DHC, while locating module ERG2/3 into LDs improved the whole metabolic flux of the post-squalene pathway. Coexpressing LD-targeted ERG2/3 and DHCR24 (generating strain SyBE_Sc01250035) improved 7-DHC production from 187.7 to 308.2 mg/L at shake-flask level. Further expressing ER-targeted module ERG1/11/24 in strain SyBE_Sc01250035 dramatically reduced squalene accumulation from 620.2 mg/L to the lowest level (by 93.8%) as well as improved 7-DHC production to the highest level (to 342.2 mg/L). Then targeting module ERG25/26/27 to LDs further increased 7-DHC titer to 360.6 mg/L, which is the highest shake-flask level production for 7-DHC ever reported. Our study not only proposes and further proves the concept of pathway compartmentalized reconstitution to regulate metabolic flux but also provides a promising chassis to produce other steroidal compounds through the post-squalene pathway.

Keywords: compartmentation, endoplasmic reticulum, lipid bodies, post-squalene pathway, 7-dehydrocholesterol, *Saccharomyces cerevisiae*

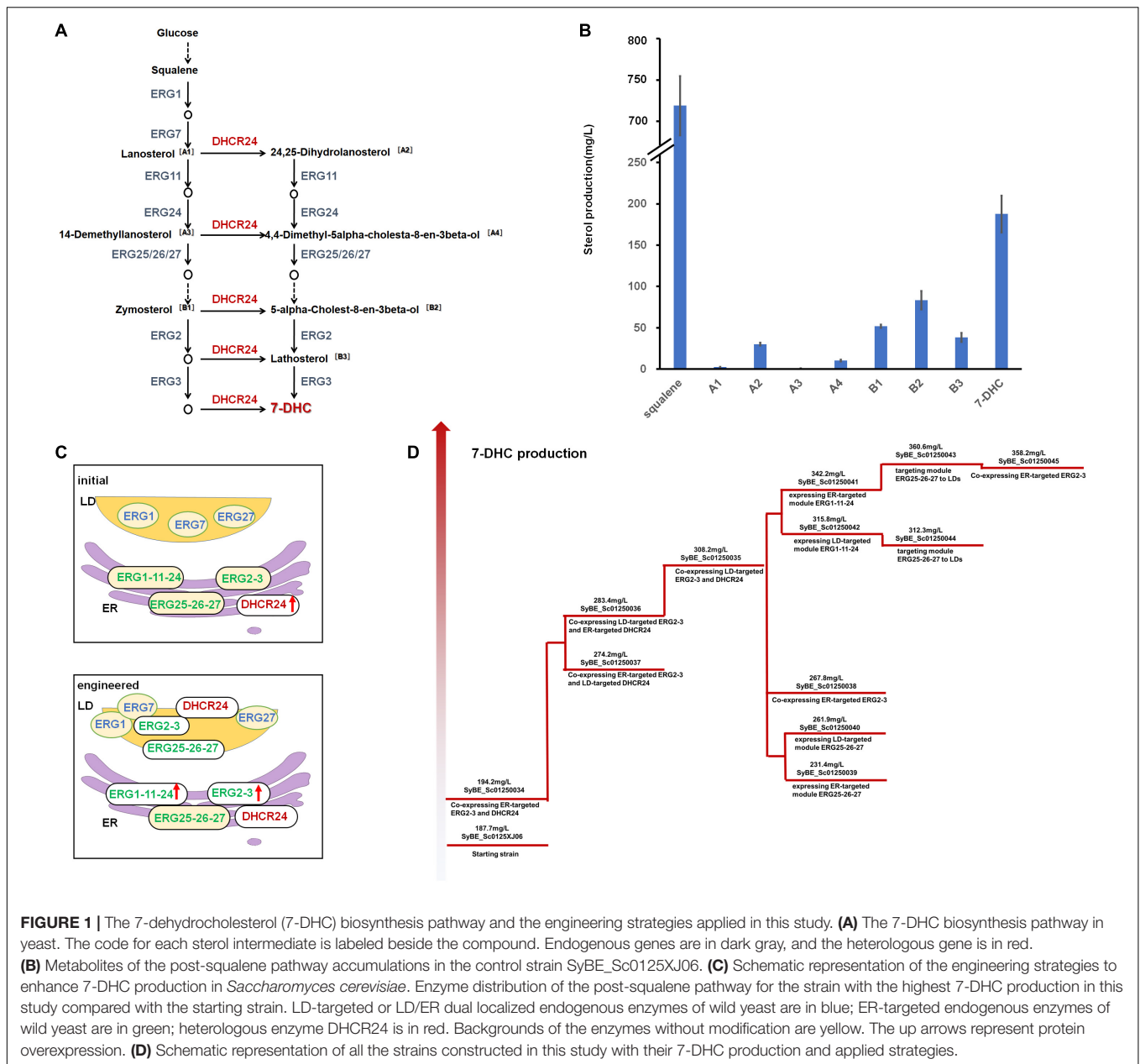
BACKGROUND

7-Dehydrocholesterol (7-DHC) is a high-valued sterol, which could be converted into vitamin D₃ (VD₃) when exposed to UV (Bendik et al., 2014). Besides being an essential nutriment, VD₃ and its derivatives [such as 25-OH-VD₃ and 1,25-(OH)₂-VD₃] are also medicines for many diseases (Bendik et al., 2014; de Sousa Almeida-Filho et al., 2017; Lu et al., 2017; Ali, 2020; D'Avolio et al., 2020; Kanstrup et al., 2020; Maghbooli et al., 2020). So far, *de novo* biosynthesis of 7-DHC has been realized in *Saccharomyces cerevisiae* by introducing heterologous Δ^{24} -dehydrocholesterol reductase (DHCR24) based on endogenous ergosterol synthesis pathway (Lang and Veen, 2011; Hohmann et al., 2012; Su et al., 2015; Guo et al., 2018), in which squalene is a key node separating the pre-squalene pathway and post-squalene pathway. The engineering approaches applied on pre-squalene pathway hardly affect the metabolic flux through the post-squalene pathway. As there is only one heterologous enzyme involved in 7-DHC synthesis (Figure 1A), therefore, the production of 7-DHC largely depends on the behavior of the post-squalene pathway. Although 7-DHC production has been greatly boosted by many metabolic engineering strategies, such as blocking the competitive ergosterol accumulation (Hohmann et al., 2012; Su et al., 2015), improving precursor supply (Lang and Veen, 2011; Su et al., 2015; Guo et al., 2018), screening the key enzyme sources (Hohmann et al., 2012; Guo et al., 2018), alleviating redox imbalance (Su et al., 2015), as well as regulating lipid metabolism (Guo et al., 2018), a large amount of post-squalene intermediates [e.g., squalene, zymosterol (B1), and 5 α -Cholest-8-en-3 β -ol (B2)] still accumulated within the producing strains, such as our previously constructed strain SyBE_Sc0125XJ06 (Guo et al., 2018; Figure 1B). In this strain, all the mevalonate (MVA) pathway genes (*ERG10*, *ERG13*, *tHMG1*, *ERG12*, *ERG8*, *ERG19*, *IDII*, and *ERG20*) were overexpressed for enhancing precursor supply; *ERG5* and *ERG6* were knocked out to block the branch pathway. Two copies of heterologous gene *DHCR24* were introduced and overexpressed under *GAL1* promoter. Notably, squalene accumulation is the biggest obstacle at the current stage. There was 187.7 mg/L of 7-DHC obtained along with 718.9 mg/L of squalene produced at shake-flask level (Figure 1B). These metabolic bottlenecks within the post-squalene pathway seriously obstruct the conversion from upstream metabolites to 7-DHC.

Balancing the expression level of the modules besides the metabolic node is a promising strategy to reduce the bottleneck of our desired pathway. There are nine ERG proteins catalyzing 16 steps of reactions within the post-squalene pathway (Figure 1A). Our previous study once tempted to tune the expression level of *DHCR24* (Guo et al., 2018) and every post-squalene proteins (Zhang et al., 2016). However, the effect of these modification on the metabolic flow of the post-squalene pathway is very limited, which pushed us to seek other solutions for this issue. Fortunately, the subcellular distribution of these ERG proteins gives us a hint of the potential solution to those metabolic bottlenecks. As shown in Figure 1C, post-squalene enzymes are not organized in one single organelle in the *S. cerevisiae* cytoplasm, but distribute between the endoplasmic reticulum (ER) and lipid bodies (LDs). To be specific, *ERG1* and *ERG27*

are found on both organelles, while *ERG7* is the only enzyme that located only in LDs (Milla et al., 2002). The rest of the ERG proteins locate in the ER (Ott et al., 2005). This distribution pattern might raise difficulties for ERG proteins to catalyze and deliver sterol intermediates, resulting in unbalanced metabolic flow and even low product yield of the desired product. Meanwhile, excess sterols generated in yeast cells are always stored in LDs in their ester forms (Zweytick et al., 2000; Jacquier and Schneiter, 2012). Ott et al. (2005) once reported the existence of sterol metabolites (e.g., B1) accumulated in LDs at significant levels in the strain with the same Δ *ERG6* background as our strain SyBE_Sc0125XJ06 (Figure 1C). These parts of sterols are hard to be catalyzed by ER-located proteins like *ERG2* for its direct substrate B1. Moreover, organelles can provide different intracellular environments for enzyme catalysis, such as different pH environments or redox states. Therefore, a certain organelle may be more conducive to the catalysis of a specific protein. It was reported that mitochondria provided a preferable environment for amorphaadiene synthase (ADS) activity, which caused enhanced amorphaadiene production when ADS was overexpressed in yeast mitochondria compared with in the cytosol (Yuan and Ching, 2016). Thus, the subcellular distribution of post-squalene enzymes might be the limiting factor for the metabolic flux of this pathway. In addition, compartmentalized reconstitution, which used to be an effective way to improve outputs of many natural products (Lin et al., 2017; Sadre et al., 2019; Yang et al., 2019; Yee et al., 2019; Jia et al., 2020; Liu et al., 2020), also would be a promising solution to boost 7-DHC titer when applied in the post-squalene pathway.

In this study, after identifying the location of the only heterologous enzyme *DHCR24* (C-24 reductase) on ER like most of the other ERG enzymes, all the ER-located proteins within the post-squalene pathway were chosen to prove the concept of pathway compartmentalized reconstitution on regulation of metabolic flux. Strain SyBE_Sc0125XJ06 with double deletion of *ERG5/ERG6* and two copies of *DHCR24* was employed as the starting strain. The whole post-squalene pathway was divided into two parts by B1, and all the ER-located enzymes were grouped into four modules: *ERG1/11/24*, *ERG25/26/27*, *ERG2/3*, and *DHCR24*. These modules were individually overexpressed on ER or in LDs (Figure 1D). Also, their effects on the production of 7-DHC as well as the accumulation of sterol intermediates were investigated, revealing an effective effort of pathway compartmentalization to pull down the metabolic flux through the post-squalene pathway. Eventually, targeting modules *ERG25/26/27*, *ERG2/3*, and *DHCR24* into LDs along with supplementing another copy of ER-located *ERG1/11/24* promoted 7-DHC production from the initial 187.7–360.6 mg/L at shake-flask level in strain SyBE_SC01250043, while the squalene accumulation was dramatically reduced by 95.5% to 32.4 mg/L. Although adding another copy of ER-located *ERG2/3* into strain SyBE_SC01250043 did not further improve the 7-DHC titer, it increased the 7-DHC ratio to 39% of the total sterols, which is 2.29-fold of the initial ratio. This study achieves the highest shake-flask level titer of 7-DHC as known, which demonstrates a promising strategy to regulate metabolic flux by pathway compartmentalized reconstitution. In



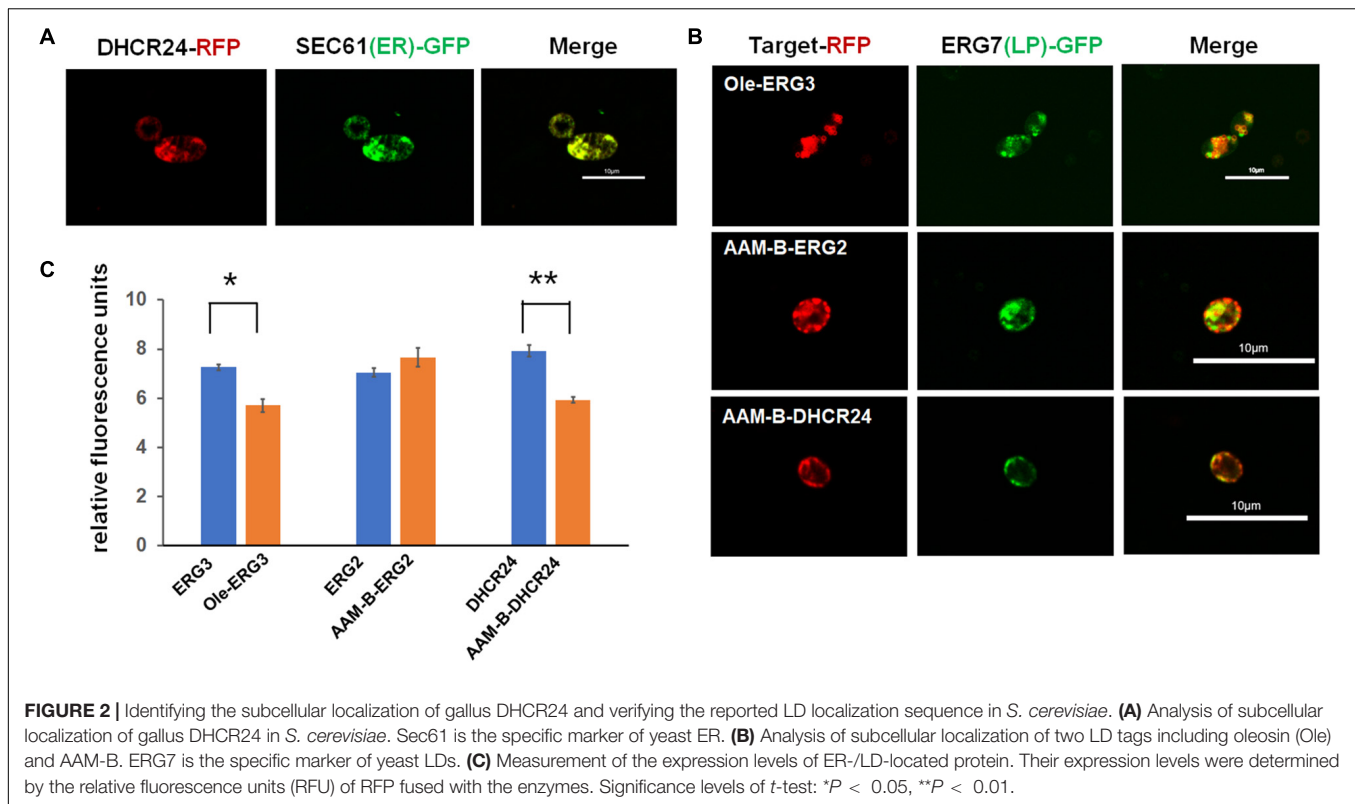
addition, sterol intermediates within the post-squalene pathway are also precursors to manufacture other valuable steroidal compounds; therefore, this study also provides an efficient chassis for microbial steroidogenesis.

RESULTS AND DISCUSSION

Identifying the Subcellular Location of the Desired Protein in *Saccharomyces cerevisiae*

A 7-DHC-producing strain SyBE_Sc0125XJ06, which was constructed in our previous study (7-DHC titer of 187.7 mg/L),

was chosen as the starting strain for pathway compartmentation. In this strain, MVA pathway genes were all overexpressed under GAL promoters (Westfall et al., 2012) to enhance precursor supply (Guo et al., 2018). GAL promoters were functioned as inducible promoters during cultivation (Westfall et al., 2012) to separate the 7-DHC production stage from the cell growth stage. In strain SyBE_Sc0125XJ06, the genes *ERG5/ERG6* were knocked out to block branch metabolic flow to ergosterol, while one copy of *gallus DHCR24*, which was controlled by *GAL1* promoter, was integrated into the *GAL1,7,10* locus (Johnston, 1987; Peng et al., 2017). As mentioned above, we have already known all the subcellular locations of the whole post-squalene proteins in *S. cerevisiae*, but not for DHCR24. DHCR24 is the only heterologous enzyme catalyzing one of the rate-limiting

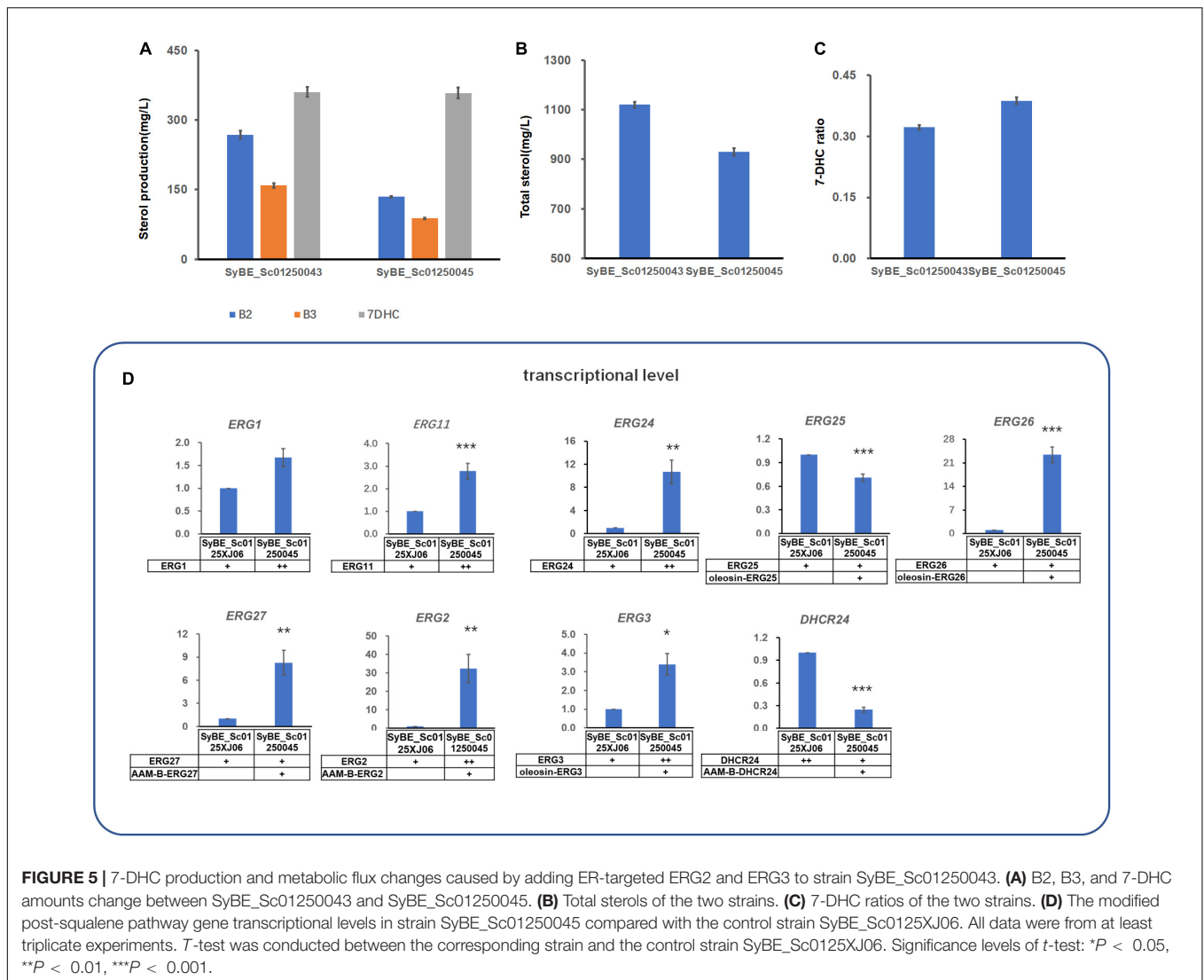


steps in the 7-DHC synthetic pathway. However, there is little research on gallus DHCR24 so far. According to Wu et al. (2004), research on human DHCR24, endogenous DHCR24, was located on the ER under basal conditions in human cells. The N-terminus of the human DHCR24 is identified as a potential transmembrane domain. This part of the sequences is predicted to partially embed in the membrane as a stem or “peduncle” rather than to traverse the membrane bilayer, which firmly anchors the protein to the membrane (Lu et al., 2012; Zerenturk et al., 2013). With a similar structure, when gallus DHCR24 (Caldwell et al., 2005) was introduced into *S. cerevisiae*, it would locate at a specific membrane structure with a high probability. However, yeasts have large and diverse membranes, making the issue on enzyme original location loss a possibility. Thus, we need to explore whether the relocating site of gallus DHCR24 in *S. cerevisiae* is still on the ER. Correspondingly, red fluorescent protein (RFP) was fused to the C-terminal of DHCR24 and coexpressed with green fluorescent protein (GFP)-linked Sec61, which was recognized as the specific marker for ER (Wilkinson et al., 1996; Kim et al., 2019). Confocal laser scanning microscopy demonstrated overlapped fluorescence signal patterns between DHCR24-RFP and Sec61-GFP (Figure 2A) proving that gallus DHCR24 is indeed located on the ER in yeast, which is consisted to DHCR24 in human cells.

As we illustrated above, the ERG protein distribution in yeast cells may cause an unbalanced metabolic flow. Since most of these proteins are mainly localized on the ER, we intended to express another copy on LDs to accelerate the delivering of intermediate metabolites. As reported, the protein oleosin from *Zea mays*

(van Rooijen and Moloney, 1995; Mullner et al., 2004; Lin et al., 2017) and the N-terminal of a putative methyltransferase AAM-B (Zehmer et al., 2008) are commonly used peptides to direct the desired enzymes to yeast LDs. These two LD-targeting sequences are usually attached to the N-terminal of the target enzymes. We chose the yeast native enzymes ERG2/ERG3 and foreign enzyme DHCR24 to verify the function of these peptides especially on proteins with original transmembrane regions responding to ER location. As demonstrated in Figure 2B, oleosin was fused to ERG3, while AAM-B tag was fused to ERG2 and DHCR24, respectively. In order to verify whether these oleosin or AAM-B tag linked proteins were expressed in LDs, RFP was fused to their C-terminals. In the meanwhile, ERG7, which is the unique sterol synthesis enzyme that only localized on LDs, was selected as the LD-specific marker and expressed along with GFP fused to its C-terminal. Both the RFP and GFP fused proteins were co-expressed in the same cell. As a result, all the images of the red fluorescence signals were mainly coincident with the corresponding green ones (Figure 2B), suggesting that oleosin and AAM-B tags could target the ER proteins onto yeast LDs.

To test if relocation of enzymes could affect the protein expression levels, all the relocated enzymes and the original ER-located enzymes were fused with RFP, and their expression levels were determined by measuring the relative fluorescence units (RFU) of these enzymes. As shown in Figure 2C, fusing with the LD-relocating sequences did not improve protein expression of these relocated proteins, indicating that further increasing 7-DHC production by relocating post-squalene proteins to LDs were likely caused by other reasons.



respectively, while introducing one copy of ER- or LD-targeted ERG1/11/24 into strain SyBE_Sc01250035 produced strains SyBE01250041 and SyBE01250042, respectively. Then a supplement of another copy of LD-expressed ERG25/26/27 into strains SyBE01250041 and SyBE01250042 obtained strains SyBE01250043 and SyBE01250044, respectively. These constructed strains were also cultivated for 100 h to measure their products by GC/MS.

PCA experiments was also conducted on the data presented in **Supplementary Table 2**. Through PCA experiments, we calculated out two principal components, Dim1 and Dim2. Except A1, A2, and B2 contributing both to Dim1 and Dim2, other sterols like squalene, B3, A3, A4, etc., contributed most to Dim1. According to the results of PCA experiments (**Figure 4A**), all the tested strains were divided into three categories, i.e., Class I for SyBE_Sc01250039 and SyBE_Sc01250040, Class III for SyBE_Sc01250042, and SyBE_Sc01250044, as well as Class II for SyBE_Sc01250041 and SyBE_Sc01250043. The differences among the strains belonging to these three classes depended

on whether ERG1/11/24 was overexpressed and where it was overexpressed, suggesting that the expression level as well as the location of ERG1/11/24 were the key points in the modification of upstream proteins for improving 7-DHC production.

In Class I, module ERG25/26/27 was overexpressed. As a result, no matter where ERG25/26/27 was located, there was still a dramatic accumulation of squalene (**Figure 4B**). Only A4 was sharply decreased (**Figure 4B**), due to overexpression of ERG25/26/27. Compared with the control strain SyBE_Sc01250035, the total sterol accumulation of SyBE_Sc01250040 as well as 7-DHC productions of strains SyBE_Sc01250039 and SyBE_Sc01250040 were both decreased, along with no improvement on the 7-DHC ratio.

In Class II, one copy of the LD-targeted ERG1/11/24 was introduced into the control strain SyBE_Sc01250035. Compared with the control strain, the accumulation of squalene declined dramatically by 78.9 and 81.1%, respectively, for strains SyBE_Sc01250042 and SyBE_Sc01250044. This part of squalene was mainly transformed into sterols upstream of B1 (**Figure 4B**).

With unchanged 7-DHC productions and decreased total sterol amounts, 7-DHC ratios were improved by 22.9%.

Different from Class II, in Class III, one copy of ER-expressed ERG1/11/24 was introduced into the control strain SyBE_Sc01250035. Compared with the Class II strains, the accumulation of squalene in Class III strains was further reduced along with decreased amounts of upstream sterols A1 and A2 as well as increased production of downstream sterols B2, B3, and 7-DHC (**Figure 4B**), suggesting that ER-expressed ERG1/11/24, but not LD-targeted ERG1/11/24, could pull the metabolic flow from upstream squalene to the downstream sterols. Since either ER-expressed or LD-targeted ERG1/11/24 could reduce squalene accumulation, we speculated that ERG1 might function well on both organelles, but ERG11/24 might be more suitable in the ER than in LDs. As a result, even though the amounts of total sterols were also lower than that of the control strain, 7-DHC production of strains SyBE_Sc01250041 and SyBE_Sc01250043 increased by 10.5% (to 342.2 mg/L) and 16.4% (to 360.6 mg/L), respectively (**Figure 4C**), along with enhanced 7-DHC ratios. The improved 7-DHC titer and ratio of strain SyBE_Sc01250043 than SyBE_Sc01250041 was due to another copy of LD-expressed ERG25/26/27. Although this modification brought no positive effect in Class I strains, it reduced the accumulation of the substrates A3 and A4, and increased the production of B1 in both Class II and Class III strains (**Figure 4B**). It was deduced that overexpressing ERG25/26/27 in LDs converted more their precursors into downstream intermediates, which could help increase 7-DHC production in some strains like SyBE_Sc01250043. Strain SyBE_Sc01250043 achieved the highest 7-DHC production at shake-flask level as was known.

Further Reducing the Metabolites of the Strain Modified by Compartmentalized Reconstitution

According to our conclusions from a former part of the study, ER-located ERG2/3 could lower some sterols downstream of B1. In order to further reduce the accumulation of sterol metabolites, one copy of ER-expressed ERG2/3 was introduced into strain SyBE_Sc01250043, generating SyBE_Sc01250045. In strain SyBE_Sc01250045, 7-DHC had no significant change to strain SyBE_Sc01250043 (**Figure 5A**). Amounts of B2 and B3, the direct precursor of ERG2 and ERG3, both decreased dramatically (**Figure 5A**), and other sterols' amounts had little change with strain SyBE_Sc01250043 (**Supplementary Table 2**). Therefore, the total sterol amounts of strain SyBE_Sc01250045 decreased (**Figure 5B**), and 7-DHC ratio increased, compared with those of strain SyBE_Sc01250043 (**Figure 5C**). The growth curves of all strains in this study were identical (**Supplementary Figure 1**). Also, the real-time quantitative PCR (QPCR) test results showed that transcription levels of most of the modified genes in strain SyBE_Sc01250045 (except *ERG1*, *ERG25*, and *DHCR24*) were increased compared with SyBE_Sc0125XJ06 (**Figure 5D**), which is one of the reasons for enhanced 7-DHC production. We speculated that the increased transcription levels of these genes may be due to the raised copy number of these genes.

TABLE 1 | *Saccharomyces cerevisiae* strains used in this study.

Strain	Description	Source
CEN.PK2-1D	<i>MATα</i> , <i>URA3-52</i> , <i>TRP1-289</i> , <i>LEU2-3,112</i> , <i>HIS3Δ1</i> , <i>MAL2-8C</i> , <i>SUC2</i>	EUROSCARF
SyBE_Sc0125 × 001	CEN.PK2-1D, <i>LEU2:BioR-ERG19-P_{GAL1,10}-ERG8</i> , <i>ADE1:tHMG1-P_{GAL1,10}-IDI1_ADE1</i> , <i>HIS3:HIS3-ERG12-P_{GAL1,10}-ERG10</i> , <i>URA3:tHMG1-P_{GAL1,10}-ERG13-URA3</i> , <i>TRP1:tHMG1-P_{GAL1,10}-ERG20-TPR1</i> , <i>GAL1,7,10:HphR ΔERG5</i> <i>GAL7,10,1:P_{GAL1}-Gg_DHCR24-T_{CYC1}</i>	Previous study
SyBE_Sc0125XJ06	SyBE_Sc0125 × 001, <i>ΔERG6:P_{GAL1}-DHCR24-T_{CYC1}-LEU2-</i>	Previous study
SyBE_Sc01250034	SyBE_Sc0125XJ06, <i>HO:URA3-P_{GAL1}-</i> <i>ERG3-T_{FBA11}-P_{GAL7}-ERG2-T_{PGK11}</i>	This study
SyBE_Sc01250035	SyBE_Sc0125 × 001, <i>ΔERG6:P_{GAL1}-AAMB-DHCR24-T_{CYC1}-</i> <i>LEU2 HO:URA3-P_{GAL1}-Oleosin-ERG3-</i> <i>T_{FBA11}-P_{GAL7}-AAMB-ERG2-T_{PGK11}</i>	This study
SyBE_Sc01250036	SyBE_Sc0125XJ06, <i>HO:URA3-P_{GAL1}-Oleosin-ERG3-</i> <i>T_{FBA11}-P_{GAL7}-AAMB-ERG2-T_{PGK11}</i>	This study
SyBE_Sc01250037	SyBE_Sc0125 × 001, <i>ΔERG6:P_{GAL1}-AAMB-DHCR24-T_{CYC1}-</i> <i>LEU2 HO:URA3-P_{GAL1}-ERG3-T_{FBA11}-</i> <i>P_{GAL7}-ERG2-T_{PGK11}</i>	This study
SyBE_Sc01250038	SyBE_Sc01250035, <i>Delta15:P_{GAL1}-</i> <i>ERG3-T_{FBA11}-P_{GAL7}-ERG2-T_{PGK11}</i>	This study
SyBE_Sc01250039	SyBE_Sc01250035, <i>Delta22:</i> <i>P_{GAL1}-ERG25-GGGGS-ERG26-T_{FBA11}-</i> <i>P_{GAL7}-ERG27-T_{PGK11}</i>	This study
SyBE_Sc01250040	SyBE_Sc01250035, <i>Delta22:P_{GAL1}-ERG25-Oleosin-ERG26-</i> <i>T_{FBA11}-P_{GAL7}-AAMB-ERG27-T_{PGK11}</i>	This study
SyBE_Sc01250041	SyBE_Sc01250035, <i>Delta22:P_{GAL1}-</i> <i>ERG1-GGGGS-ERG11-T_{FBA11}-P_{GAL7}-</i> <i>ERG24-T_{PGK11}</i>	This study
SyBE_Sc01250042	SyBE_Sc01250035, <i>Delta22:P_{GAL1}-</i> <i>ERG1-Oleosin-ERG11-T_{FBA11}-P_{GAL7}-</i> <i>AAMB-ERG24-T_{PGK11}</i>	This study
SyBE_Sc01250043	SyBE_Sc01250040, <i>Delta15:P_{GAL1}-</i> <i>ERG1-GGGGS-ERG11-T_{FBA11}-P_{GAL7}-</i> <i>ERG24-T_{PGK11}</i>	This study
SyBE_Sc01250044	SyBE_Sc01250040, <i>Delta15:P_{GAL1}-</i> <i>ERG1-Oleosin-ERG11-T_{FBA11}-P_{GAL7}-</i> <i>AAMB-ERG24-T_{PGK11}</i>	This study
SyBE_Sc01250045	SyBE_Sc01250043, <i>Tau3:KANMX-P_{GAL1}-ERG3-T_{FBA11}-</i> <i>P_{GAL7}-ERG2-T_{PGK11}</i>	This study
SyBE_Sc0125P001	CEN.PK2-1D, PRS425K- <i>P_{GAL1}-Gg_DHCR24-RFP-T_{FBA1}</i> , <i>PRS416-P_{GAL1}-SEC61-GFP-T_{FBA1}</i>	This study
SyBE_Sc0125P002	CEN.PK2-1D, PRS425K- <i>P_{GAL1}-AAMB-DHCR24-RFP-T_{FBA1}</i> , <i>PRS416-P_{GAL1}-ERG7-GFP-T_{FBA1}</i>	This study
SyBE_Sc0125P003	CEN.PK2-1D, PRS425K- <i>P_{GAL1}-AAMB-ERG2-RFP-T_{FBA1}</i> , <i>PRS416-P_{GAL1}-ERG7-GFP-T_{FBA1}</i>	This study
SyBE_Sc0125P004	CEN.PK2-1D, PRS425K- <i>P_{GAL1}-Oleosin-ERG3-RFP-T_{FBA1}</i> , <i>PRS416-P_{GAL1}-ERG7-GFP-T_{FBA1}</i>	This study

Besides, another reason for raised transcription levels may be enzymes relocated to the LDs. To be noticed, in the former study, when SyBE_Sc01250035 was introduced the same module (ER-located ERG2/3), the overall metabolic flux reduced, while only squalene increased in strain SyBE_Sc01250038. The reason why introducing the same ER-expressed ERG2/3 in different strains had a so different impact on metabolic flux still needs to be explained. In the meanwhile, since we presumed that ER-located ERG3 might have insufficient catalytic ability due to the increased accumulation of B3 in strains SyBE_Sc01250034 and SyBE_Sc01250037, other heterologous ERG3s should be screened and introduced into the 7-DHC-producing strain. In addition, a more delicate compartmentation test on those key modules like ERG2/3 and ERG1/11/24 should be also conducted by targeting a single ERG protein to one organelle at one time. Besides, we can further rearrange the LD-located enzymes like ERG7 to ER in the strains constructed in this study and investigate their effects on the accumulation of 7-DHC and other sterol intermediates.

CONCLUSION

In this study, subcellular locations of post-squalene pathway enzymes were rearranged in order to improve the unbalanced metabolic flow and low product yield caused by the dual organelle locations. All the ER-located enzymes of the post-squalene pathway were grouped into four modules: ERG1/11/24, ERG25/26/27, ERG2/3, and DHCR24. These modules were overexpressed on ER or on LDs. We subsequently rearranged the locations of enzymes downstream and upstream of B1. We conducted PCA experiments to classify the strains and analyzed the metabolic flux of strains in each class. We also obtain some strains in which 7-DHC production and 7-DHC ratio both dramatically increased through rearranging the post-squalene pathway enzymes. Eventually, targeting modules ERG25/26/27 and ERG2/3 into LDs along with supplementing another copy of ER-located ERG1/11/24 promoted 7-DHC production from the initial 187.7–360.6 mg/L at shake-flask level in strain SyBE_SC01250043, while the squalene accumulation was dramatically reduced by 95.5% to 32.4 mg/L. Although adding another copy of ER-located ERG2/3 into strain SyBE_SC01250043 did not improve the 7-DHC titer, the 7-DHC ratio further increased to 39% of the total sterols, which is 2.32-fold of the initial ratio. This study achieves the highest shake-flask level titer of 7-DHC as was known, which demonstrated that compartmentalized reconstitution of the post-squalene pathway was an efficient way to optimize metabolic flux in the 7-DHC pathway and promote 7-DHC production and ratio.

MATERIALS AND METHODS

Strains, Media, and Cultivation

All *E. coli* and *S. cerevisiae* strains used in this work are summarized in **Table 1**. All modified yeast strains were derived from CEN.PK2-1D. *E. coli* DH5 α was used for molecular cloning. *E. coli* was grown in Luria broth (LB) medium containing 50 $\mu\text{g ml}^{-1}$ of ampicillin or 50 $\mu\text{g ml}^{-1}$ of kanamycin for construction

of plasmids and strains. Solid synthetic complete (SC) medium (0.67% yeast nitrogen base, amino acid supplements, and 2% glucose) lacking the appropriate nutrient component were used to select recombinational yeast strains. Shake-flask fermentation was performed in modified YPD medium [2% peptone, 1% yeast extract, 4% glucose, and 1% D-(+)-galactose] at 30°C.

For shake-flask fermentation, constructed strains were cultured and purified on an SC plate. A single colony was cultivated in 5 ml of YPD medium overnight at 30°C, and the culture was transferred into 40 ml of modified YPD when cells entered the mid-exponential phase. The initial glucose concentration in YPD medium was 40 g/L and OD₆₀₀ was 0.2. D-galactose (10 g/L) was added into the media at the beginning of fermentation for inducing GAL promoters of recombinational strains. Shake-flask fermentation lasted for 100 h.

Construction of Plasmids and Strains

For constructing ERG2, ERG3, and DHCR24 relocating strains, ERG2 and ERG3 were fused with LD-targeting sequence AAM-B and oleosin to their 3'-terminuses individually by OE-PCR (**Supplementary Figure 2**). Modified genes AAM-B-ERG2 and oleosin-ERG3 were cloned into expression cassettes containing GAL7 or GAL1 promoter, which were built in our previous study. The original genes ERG2 and ERG3 were also cloned into the corresponding expression cassettes for control. Expression cassettes containing the desired genes "TDH2t-GAL1p-gene1-FBA1t" and "FBA1t-GAL7p-gene2-PGK1t" were then PCR amplified with 20-bp overlap to plasmid PRS425K and flanking specific restriction enzyme sites at one terminus, and the two expression cassettes also had a 20-bp overlap at their adjacent ends. The two resulting amplicons were assembled into linearized vector PRS425K with SE Seamless Cloning and Assembly Kit (Beijing Zoman Biotechnology). The recombinant modules containing two gene expression cassettes were released from plasmids by corresponding restriction enzymes cutting at the 5' and 3' terminus of the whole modules as genomic integration fragment (no. 1). Genomic sequences covering around 700 bp upstream of the desired integration site, selection marker, and terminator TDH2t (no selection marker if the integration was in the CRISPR method, when ERG2 and ERG3 were integrated in the YPRC Δ 15 locus) were amplified from *S. cerevisiae* genome and joined by overlap PCR. The resulting amplicon was ligated into a PEAZY-blunt vector, and the recombinant plasmids were digested by restriction enzymes to yield the left arm fragment of the homologous recombination (no. 2). The right arm fragment (no. 3) was obtained in the same way as terminator PGK1t and 700-bp downstream of the desired integration locus. The three fragments above were transformed using the LiAc/SS carrier DNA/PEG method. For integration of ERG2/ERG3 in YPRC Δ 15 locus, the CRISPR method was used. Two complementary primers from the target sequence YPRC Δ 15 were annealed and ligated into CRISPR plasmid (carrying cas9 and incomplete gRNA), generating the complete guide RNA. The resulting CRISPR plasmid was transformed with the three recombination fragments above. The DHCR24 expression module and the left/right arm fragments of homologous recombination were obtained from our previous study and

integrated into genome *ERG6* locus in a similar way. For constructing *ERG1*, *ERG11*, *ERG24*, *ERG25*, *ERG26*, and *ERG27* overexpressing or relocalizing strains, the similar molecular manipulation strategy was applied except two differences: (1) According to Lin et al. (2017), oleosin sequence could relocalize two proteins into the LDs simultaneously when proteins fused to its 5'- and 3'-terminus. *ERG1*, oleosin, and *ERG11* were amplified and combined by OE-PCR (Supplementary Figure 1), the resulting amplicons were recombined into the *GAL1p* expression cassette. In order to be consistent with the relocalization method, *ERG1* and *ERG11* used DNA linker GGGGS to become a fused protein for their overexpression experiment. *ERG25* and *ERG26* overexpressing or relocalizing strains were also constructed in the same way. (2) The right arm fragment of the homologous recombination for *ERG* genes integrating upstream of B1 was different. Expression cassette “*FBA1t-GAL7p-gene-PGK1t*” and about 700 bp of overlap of downstream, the desired genomic integration site was joined by OE-PCR as the right arm fragment to reduce the number of recombination fragments to three.

Extraction and Analysis of Sterols

Sterol extraction was performed as previously described (Guo et al., 2018). Yeast cells were harvested by centrifugation at 12,000 rpm for 2 min after fermentation process and boiled in 3 N HCl for 5 min to break the cell wall. Cells were pelleted and washed by distilled water to remove the remaining HCl. After neutralizing by NaOH, saponification reaction of cells was carried out in 3 M NaOH-methanol solution at 60°C for 4 h. n-Hexane and silica sand were added for sterol extraction with vortex. The n-hexane phase was collected and dried by a centrifugal vacuum evaporator. N-methyl-N-(trimethylsilyl) trifluoroacetamide (MSTFA) was used to derivatize the obtained sterols (30°C for h) and samples were ready for GC-MS analysis.

Sterols were separated and analyzed by GCMS-QP2020 (SHIMADZU, Japan) using a DB-5 fused-silica capillary column (30 m × 0.25 mm i.d., film thickness 0.25 μm, J&W Scientific, CA). Mass spectra ranged at 50–800 m/z, and helium was used as the carrier gas. Operating conditions were inlet temperature 260°C, initial temperature 70°C for 2 min then ramp 30°C/min to 250°C then ramp 10°C/min to 280°C and held for 15 min. Finally, the temperature increased to 290°C at 5°C/min and was held for 5 min. Sterol standards (squalene, A1, A2, B3, B1, 7-DHC, etc.) were purchased from Sigma-Aldrich (United States).

Principal Component Analysis

All visualizations of principal component analysis (Pearson, 2010) were performed in the R package FactoMineR (Lê et al., 2008).

Protein Expression Level Analysis

Strains were cultured in SC-leu medium with 20 g/L of galactose for 60 h. A plate reader (SpectraMAX M2, Molecular Devices)

used with a 587-nm excitation filter and a 610-nm emission filter was for measurement of the fluorescence of RFP.

Genes Transcriptional Analysis

The real-time quantitative PCR (QPCR) process was similar to our published article (Guo et al., 2018). Strains were cultured in a shake flask for 30 h (ethanol consumption phase) and then harvested. Total RNA extraction, reverse transcription, and QPCR were carried out by Apexbio Inc. (China). The gene *ALG9* was used for normalization.

DATA AVAILABILITY STATEMENT

The original contributions presented in the study are included in the article/Supplementary Material, further inquiries can be directed to the corresponding author/s.

AUTHOR CONTRIBUTIONS

X-JG and YW conceived the study as well as participated in the strain construction and carried out the molecular genetic studies. X-JG and W-HX conducted the fermentation. M-DY, G-RZ, and Y-JY participated in the design and coordination of the study as well as helped draft the manuscript. YW supervised the whole research and revised the manuscript. All authors read and approved the final manuscript.

FUNDING

This work was supported by the National Natural Science Foundation of China (32071415 and 21621004).

ACKNOWLEDGMENTS

We are grateful to Prof. Fei Guo and Xinyu Chen from the College of Intelligence and Computing, Tianjin University, for helping in conducting the PCA analysis. We also thank Dr. Bo-xuan Zeng from the Tianjin University for kindly providing some *S. cerevisiae* chassis.

SUPPLEMENTARY MATERIAL

The Supplementary Material for this article can be found online at: <https://www.frontiersin.org/articles/10.3389/fmicb.2021.663973/full#supplementary-material>

REFERENCES

Ali, N. (2020). Role of vitamin D in preventing of COVID-19 infection, progression and severity. *J. Infect. Public Health* 13, 1373–1380. doi: 10.1016/j.jiph.2020.06.021

Bendik, I., Friedel, A., Roos, F. F., Weber, P., and Eggersdorfer, M. (2014). Vitamin D: a critical and essential micronutrient for human health. *Front. Physiol.* 5:248.

Caldwell, R. B., Kierzek, A. M., Arakawa, H., Bezzubov, Y., Zaim, J., Fiedler, P., et al. (2005). Full-length cDNAs from chicken bursal lymphocytes to facilitate gene function analysis. *Genome Biol.* 6:R6.

- D'Avolio, A., Avataneo, V., Manca, A., Cusato, J., De Nicolo, A., Lucchini, R., et al. (2020). 25-hydroxyvitamin D concentrations are lower in patients with positive PCR for SARS-CoV-2. *Nutrients* 12:1359. doi: 10.3390/nu12051359
- de Sousa Almeida-Filho, B., De Luca Vespoli, H., Pessoa, E. C., Machado, M., Nahas-Neto, J., and Nahas, E. A. P. (2017). Vitamin D deficiency is associated with poor breast cancer prognostic features in postmenopausal women. *J. Steroid Biochem. Mol. Biol.* 174, 284–289. doi: 10.1016/j.jsbmb.2017.10.009
- Guo, X. J., Xiao, W. H., Wang, Y., Yao, M. D., Zeng, B. X., Liu, H., et al. (2018). Metabolic engineering of *Saccharomyces cerevisiae* for 7-dehydrocholesterol overproduction. *Biotechnol. Biofuels* 11:192.
- Hohmann, H. P., Lehmann, M., and Merkmann, M. (2012). *Production of Non-Yeast Sterols by Yeast*. US Patent, 20120231495. Washington, DC: U.S. Patent and Trademark Office.
- Jacquier, N., and Schneider, R. (2012). Mechanisms of sterol uptake and transport in yeast. *J. Steroid Biochem. Mol. Biol.* 129, 70–78. doi: 10.1016/j.jsbmb.2010.11.014
- Jia, H., Chen, T., Qu, J., Yao, M., Xiao, W., Wang, Y., et al. (2020). Collaborative subcellular compartmentalization to improve GPP utilization and boost sabinene accumulation in *Saccharomyces cerevisiae*. *Biochem. Eng. J.* 164:107768. doi: 10.1016/j.bej.2020.107768
- Johnston, M. (1987). A model fungal gene regulatory mechanism—the GAL genes of *Saccharomyces cerevisiae*. *Microbiol. Rev.* 51, 458–476. doi: 10.1128/mmb.51.4.458-476.1987
- Kanstrup, C., Teilmann, D., Rejnmark, L., Biggaard, J. V., Eiken, P., Kroman, N., et al. (2020). 25-hydroxyvitamin D at time of breast cancer diagnosis and breast cancer survival. *Breast Cancer Res. Treat* 179, 699–708. doi: 10.1007/s10549-019-05486-4
- Kim, J. E., Jang, I. S., Son, S. H., Ko, Y. J., Cho, B. K., Kim, S. C., et al. (2019). Tailoring the *Saccharomyces cerevisiae* endoplasmic reticulum for functional assembly of terpene synthesis pathway. *Metab. Eng.* 56, 50–59. doi: 10.1016/j.ymben.2019.08.013
- Lang, C., and Veen, M. (2011). *Preparation of 7-Dehydrocholesterol and/or the Biosynthetic Intermediates and/or Secondary Products Thereof in Transgenic Organisms*. US Patent 12607017. Washington, DC: U.S. Patent and Trademark Office.
- Lê, S., Josse, J., and Husson, F. (2008). FactoMineR: an Rpackage for multivariate analysis. *J. Stat. Softw.* 25, 1–18.
- Lin, J. L., Zhu, J., and Wheeldon, I. (2017). Synthetic protein scaffolds for biosynthetic pathway colocalization on lipid droplet membranes. *ACS Synth. Biol.* 6, 1534–1544. doi: 10.1021/acssynbio.7b00041
- Liu, G. S., Li, T., Zhou, W., Jiang, M., Tao, X. Y., Liu, M., et al. (2020). The yeast peroxisome: a dynamic storage depot and subcellular factory for squalene overproduction. *Metab. Eng.* 57, 151–161. doi: 10.1016/j.ymben.2019.11.001
- Lu, G., Li, J., Chu, J., Jin, S., Fu, Z., Miao, D., et al. (2017). 1,25(OH)₂D₃ deficiency increases TM40D tumor growth in bone and accelerates tumor-induced bone destruction in a breast cancer bone metastasis model. *Biomed. Pharmacother.* 95, 1033–1039. doi: 10.1016/j.biopha.2017.09.018
- Lu, X., Li, Y., Liu, J., Cao, X., Wang, X., Wang, D., et al. (2012). The membrane topological analysis of 3β-hydroxysteroid-Δ²⁴ reductase (DHCR24) on endoplasmic reticulum. *J. Mol. Endocrinol.* 48, 1–9. doi: 10.1530/jme-11-0132
- Maghbooli, Z., Sahraian, M. A., Ebrahimi, M., Pazoki, M., Kafan, S., Tabriz, H. M., et al. (2020). Vitamin D sufficiency, a serum 25-hydroxyvitamin D at least 30 ng/mL reduced risk for adverse clinical outcomes in patients with COVID-19 infection. *PLoS One* 15:e0239799. doi: 10.1371/journal.pone.0239799
- Milla, P., Athenstaedt, K., Viola, F., Oliaro-Bosso, S., Kohlwein, S. D., Daum, G., et al. (2002). Yeast oxidosqualene cyclase (Erg7p) is a major component of lipid particles. *J. Biol. Chem.* 277, 2406–2412. doi: 10.1074/jbc.m104195200
- van Rooijen, G. J., and Moloney, M. M. (1995). Structural requirements of oleosin domains for subcellular targeting to the oil body. *Plant Physiol.* 109, 1353–1361. doi: 10.1104/pp.109.4.1353
- Mullner, H., Zweytick, D., Leber, R., Turnowsky, F., and Daum, G. (2004). Targeting of proteins involved in sterol biosynthesis to lipid particles of the yeast *Saccharomyces cerevisiae*. *Biochim. Biophys. Acta* 1663, 9–13. doi: 10.1016/j.bbamem.2004.03.001
- Ott, R. G., Athenstaedt, K., Hrastnik, C., Leitner, E., Bergler, H., and Daum, G. (2005). Flux of sterol intermediates in a yeast strain deleted of the lanosterol C-14 demethylase Erg11p. *Biochim. Biophys. Acta* 1735, 111–118. doi: 10.1016/j.bbali.2005.05.003
- Pearson, K. (2010). LIII. On lines and planes of closest fit to systems of points in space. The London, Edinburgh, and Dublin. *Philos. Mag. J. Sci.* 2, 559–572. doi: 10.1080/14786440109462720
- Peng, B., Plan, M. R., Carpenter, A., Nielsen, L. K., and Vickers, C. E. (2017). Coupling gene regulatory patterns to bioprocess conditions to optimize synthetic metabolic modules for improved sesquiterpene production in yeast. *Biotechnol. Biofuels* 10:43.
- Sadre, R., Kuo, P., Chen, J., Yang, Y., Banerjee, A., Benning, C., et al. (2019). Cytosolic lipid droplets as engineered organelles for production and accumulation of terpenoid biomaterials in leaves. *Nat. Commun.* 10:853.
- Su, W., Xiao, W. H., Wang, Y., Liu, D., Zhou, X., and Yuan, Y. J. (2015). Alleviating redox imbalance enhances 7-dehydrocholesterol production in engineered *Saccharomyces cerevisiae*. *PLoS One* 10:e0130840. doi: 10.1371/journal.pone.0130840
- Westfall, P. J., Pitera, D. J., Lenihan, J. R., Eng, D., Woolard, F. X., Regentin, R., et al. (2012). Production of amorphadiene in yeast, and its conversion to dihydroartemisinic acid, precursor to the antimalarial agent artemisinin. *Proc. Natl. Acad. Sci. U.S.A.* 109, E111–E118.
- Wilkinson, B. M., Critchley, A. J., and Stirling, C. J. (1996). Determination of the transmembrane topology of yeast Sec61p, an essential component of the endoplasmic reticulum translocation complex. *J. Biol. Chem.* 271, 25590–25597. doi: 10.1074/jbc.271.41.25590
- Wu, C., Miloslavskaya, I., Demontis, S., Maestro, R., and Galaktionov, K. (2004). Regulation of cellular response to oncogenic and oxidative stress by Seladin-1. *Nature* 432:640. doi: 10.1038/nature03173
- Yang, K., Qiao, Y., Li, F., Xu, Y., Yan, Y., Madzak, C., et al. (2019). Subcellular engineering of lipase dependent pathways directed towards lipid related organelles for highly effectively compartmentalized biosynthesis of triacylglycerol derived products in *Yarrowia lipolytica*. *Metab. Eng.* 55, 231–238. doi: 10.1016/j.ymben.2019.08.001
- Yee, D. A., Denicola, A. B., Billingsley, J. M., Creso, J. G., Subrahmanyam, V., and Tang, Y. (2019). Engineered mitochondrial production of monoterpenes in *Saccharomyces cerevisiae*. *Metab. Eng.* 55, 76–84. doi: 10.1016/j.ymben.2019.06.004
- Yuan, J., and Ching, C. B. (2016). Mitochondrial acetyl-CoA utilization pathway for terpenoid productions. *Metab. Eng.* 38, 303–309. doi: 10.1016/j.ymben.2016.07.008
- Zehmer, J. K., Bartz, R., Liu, P., and Anderson, R. G. (2008). Identification of a novel N-terminal hydrophobic sequence that targets proteins to lipid droplets. *J. Cell Sci.* 121, 1852–1860. doi: 10.1242/jcs.012013
- Zerenturk, E. J., Sharpe, L. J., Ikonen, E., and Brown, A. J. (2013). Desmosterol and DHCR24: unexpected new directions for a terminal step in cholesterol synthesis. *Prog. Lipid Res.* 52, 666–680. doi: 10.1016/j.plipres.2013.09.002
- Zhang, W. Q., Xiao, Z., Xiao, W. H., and Wang, Y. (2016). Effect of post-squalene genes on the synthesis of 7-dehydrocholesterol in the artificial *Saccharomyces cerevisiae*. *China Biotechnol.* 36, 39–50.
- Zweytick, D., Leitner, E., Kohlwein, S. D., Yu, C., Rothblatt, J., and Daum, G. (2000). Contribution of Are1p and Are2p to steryl ester synthesis in the yeast *Saccharomyces cerevisiae*. *Eur. J. Biochem.* 267, 1075–1082. doi: 10.1046/j.1432-1327.2000.01103.x

Conflict of Interest: The authors declare that the research was conducted in the absence of any commercial or financial relationships that could be construed as a potential conflict of interest.

Copyright © 2021 Guo, Yao, Xiao, Wang, Zhao and Yuan. This is an open-access article distributed under the terms of the Creative Commons Attribution License (CC BY). The use, distribution or reproduction in other forums is permitted, provided the original author(s) and the copyright owner(s) are credited and that the original publication in this journal is cited, in accordance with accepted academic practice. No use, distribution or reproduction is permitted which does not comply with these terms.